Colloid Polym Sci (2007) 285:1369–1376
DOI 10.1007/s00396-007-1695-8

ORIGINAL CONTRIBUTION

Synthesis and self-assembly of comb-like amphiphilic copolymer poly(maleic anhydride-*alt*-stearyl methacrylate)-*b*-poly(stearyl methacrylate)

Junfeng Zhou · Li Wang · Qiang Yang ·
Xiaochen Dong · Haojie Yu

Received: 5 December 2006 / Accepted: 8 May 2007 / Published online: 4 July 2007

Abstract Comb-like amphiphilic block copolymers of maleic anhydride (MA) and stearyl methacrylate (SMA) were prepared through the reversible-addition-fragmentation-transfer polymerization. The resultant copolymers were characterized by gel permeation chromatograph and ^{1}H NMR. The aggregation behaviors of P(MA-*alt*-SMA)-*b*-PSMA were investigated in tetrahydrofuran/water. It is of great interest that the aggregates with different morphologies and dimensions could be obtained by adjusting the polymer concentration, water content, and pH. The dimension and structure of these aggregates were investigated by transmission electron microscopy and dynamic light scattering. The effect of the copolymer–solvent interaction on these aggregations was discussed.

Keywords Self-assembly · Comb-like amphiphilic copolymer · Stearyl methacrylate · Maleic anhydride

Introduction

It is well known that block copolymers in block-selective solvent can form colloidal micelles or aggregates as a result of the association of the insoluble blocks [1–12]. Recently, a variety of various morphologies including spheres, large compound micelles, rods, and tubules have been discovered and have drawn much attention; therefore, it is of great interest for emerging nanomaterials and nanotechnologies such as microreactors, microcapsules, drug delivery systems, and encapsulation of various kinds of guest molecules [13–17]. The aggregation architecture can be altered by controlling a great number of parameters such as temperature, solvent, concentration [18], solvent composition, water content [19], pH [20], and other factors [21].

As a novel polymerization approach, the reversible-addition-fragmentation-transfer (RAFT) polymerization has been attracting increasing interest recently because it furnishes control over the resultant polymers and can form well-defined and predictable multicomponent polymer structures. Up to now, the RAFT reaction has been successfully applied to the synthesis of macromolucular architectures such as comb, gradient, star, and block copolymers [22–26]. Recently, many studies have focused on the radical copolymerization of maleic anhydride (MA) and vinyl monomer by the RAFT polymerization [27–30]. For example, Li et al. [27] prepared a block copolymer with alternating MA/styrene segments and polystyrene segments and studied the self-assembly of the corresponding hydrolyzed amphiphilic product in water. Li et al. [28] also reported on the synthesis of a diblock copolymer containing a block of alternately structured MA with 4-vinyl benzyl chloride and a polyvinylbenzyl chloride block. It was found that this copolymer can form stable inverse micelles in tetrahydrofuran (THF) after the MA moieties were reacted with 2-mercaptoethyl amine. However, the studies mentioned above did not focus on the synthesis and self-assembly of block copolymers having MA/methacrylate segments and methacrylate segments.

In our previous work, we had synthesized P[stearyl methacrylate (SMA)-co-MA] and their derivants and

---

J. Zhou · L. Wang (✉) · Q. Yang · X. Dong · H. Yu
State Key Laboratory of Chemical Engineering,
Zhejiang University,
Hangzhou 310027, People's Republic of China
e-mail: opl_wl@zju.edu.cn

Scheme 1 Synthesis procedures of BTBA and P(MA-*alt*-SMA)-*b*-PSMA

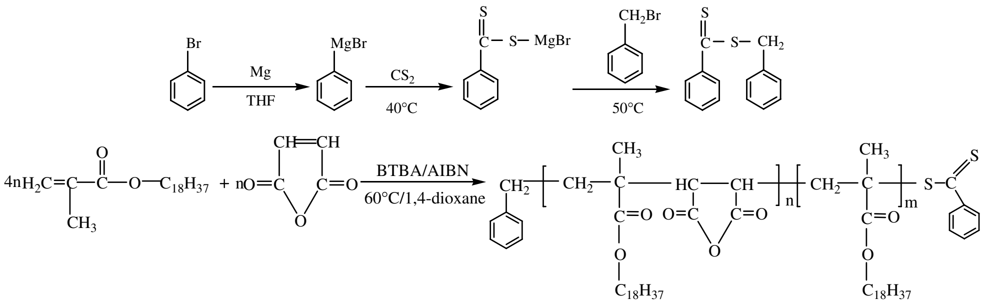

investigated their self-assembly behaviors in selective solvents [8, 9]. Here, we demonstrate that a novel amphiphilic comb-like block copolymer P(MA-*alt*-SMA)-*b*-PSMA having alternating segments can be synthesized successfully via the RAFT polymerization. Moreover, SMA is a comb-like molecule and has a pendent long alkyl side chain [31]. It is well-known that comb-like polymers can provide unique opportunities to be used as an effective barrier to protein adsorption or to generate hydrophobic surfaces of polymer film for applications in the areas of adhesion, friction, membrane transport, and biocompatibility [32, 33]. Furthermore, the synthesis and self-assembly of amphiphilic comb-like copolymers were recently studied extensively due to their interesting properties [34, 35], so the synthesis and aggregating behaviors of the novel comb-like block copolymer P(MA-*alt*-SMA)-*b*-PSMA should be worth examining in detail for potential applications. Herein, we report on the synthesis and characterization of P(MA-*alt*-SMA)-*b*-PSMA and study the self-assembly behaviors of the resultant polymers in THF/water.

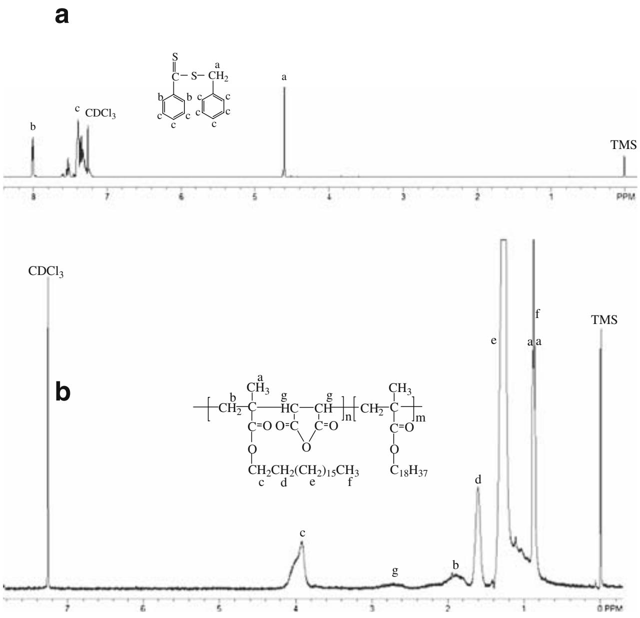

Fig. 1 ^{1}H NMR spectra of BTBA (**a**) and P(MA-*alt*-SMA)-*b*-PSMA (**b**)

Experimental

Materials

MA, SMA, 2,2′-azo-diisobutyronitrile (AIBN), 1,4-dioxane, carbon disulfide, chloroform, hexane, sodium hydroxide, acetone, methanol, magnesium sulfate, neutral alumina, petroleum ether, and dichloromethane were all purchased from Shanghai No.1 Chemical Reagent Factory. MA was recrystallized in chloroform before use. AIBN was recrystallized twice before use. SMA was treated with the literature method [36]. All other reagents were of analytical grade and used as received. Benzyl dithiobenzoate (BTBA) was prepared by the literature method [37].

Synthesis of comb-like block copolymers of P(MA-*alt*-SMA)-*b*-PSMA

In a typical RAFT synthesis, MA (0.2451 g, 2.50 mmol), SMA (3.3857 g, 10.00 mmol), BTBA (0.0125 g,

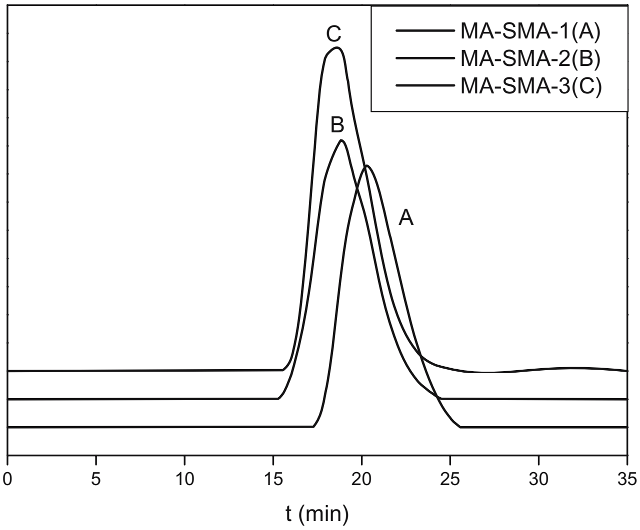

Fig. 2 GPC traces of MA–SMA copolymers obtained via RAFT polymerization. RAFT reaction time: 90 min (*A*), 180 min (*B*), and 360 min (*C*)

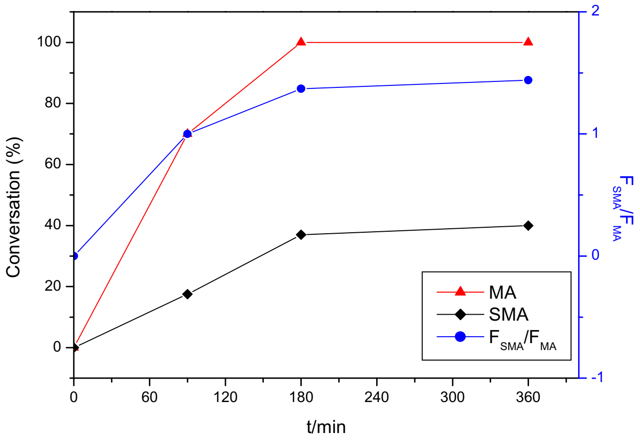

Fig. 3 Variation of monomer conversion for MA and SMA monomers and their consumed molar ratio (F_{SMA}/F_{MA}) with the polymerization time. SMA-MA copolymerization condition: $[SMA]_0$= 0.83 mol/l; $[MA]_0$=0.21 mol/l; $[BTBA]_0$=0.004 mol/l; $[AIBN]_0$= 0.002 mol/l; T=60 °C

0.05 mmol), AIBN (0.0042 g, 0.025 mmol) (100:400:2:1 in molar ratio), and 1,4-dioxane (12.0 ml) were added into a series of a 20-ml glass flask with a magnetic stirrer, followed by a freeze–vacuum–thaw cycle three times [27]. The tubes were sealed under vacuum and immersed in oil baths thermostated at 60 °C. At a prescribed time interval (90, 180, or 360 min), these tubes were taken out in succession and cooled in ice water to stop the polymerization. The copolymer products were precipitated in excess methanol. The polymers were purified by using acetone as the nonsolvent for P(MA-*alt*-SMA)-*b*-PSMA copolymer and as the solvent for homopolymer contamination at 25 °C.

Self-assembly of amphiphiles

The block copolymer P(MA-*alt*-SMA)-*b*-PSMA was first dissolved in THF at a desired concentration. Deionized water was then added at a rate of 0.5 wt.% per minute to the above copolymer solutions with vigorous stirring to induce the self-assembly. The effects of the polymer concentration, water content, and pH on the self-assembly of P(MA-*alt*-SMA)-*b*-PSMA were mainly investigated.

The polymer concentration The polymer concentrations were maintained at 0.05 and 0.2 wt.%, respectively, in THF/water 90:10 (*w*/*w*).

Water content In the system of P(MA-*alt*-SMA)$_{50}$-*b*-PSMA$_{30}$/THF, water content was varied between 5 and 30 wt.% at the polymer concentration of 0.1 wt.%.

pH In the system of P(MA-*alt*-SMA)$_{50}$-*b*-PSMA$_{30}$/THF, different amounts of HCl or NaOH were added (as aqueous solutions) to each of the above solutions. Subsequently, deionized water was added dropwise to the copolymer solution with stirring. The final pH values of the solutions were 4.0, 5.8, and 12.0, respectively, at the polymer concentration of 0.1 wt.% in THF/water 90:10 (*w*/*w*).

Finally, the self-assembly solutions were deposited for 3 h before measurement. Samples for transmission electron microscopy (TEM) measurement were prepared by aerosol spraying a drop of self-assembly solution (ca. 10 µl) on the 200-mesh gilder copper TEM grids and air-dried before introduction into TEM.

Characterizations

^{1}H NMR spectra of products were recorded with a Bruker 400 MHz Advance2B NMR spectrometer in $CDCl_3$, using TMS as the standard. The molecular weight and molecular weight distribution of the copolymers were determined on a Waters 201 gel permeation chromatograph (GPC) with laser scattering detector and ultrastyragel column with pore sizes of 10^3–10^5 Å. The eluent was THF at a flow rate of 1.0 ml/min. A detection wavelength of 632.8 nm and the refraction index increment value of the polymer solutions dn/dc=0.20 were used for laser scattering detection. TEM micrographs were obtained on a JEOL model 1200EX instrument operated at an accelerating voltage at 160 kV. Light scattering experiments were performed on a Malvern Zetasizer 3000HSA zeta potential and laser nanometer particle size analyzer equipped with a He–Ne laser

Table 1 Molecular weight, molecular weight distribution, and the composition of MA–SMA copolymers obtained via the RAFT polymerization

Copolymer	Time/min	M_n^a	M_w/M_n^a	SMA in copolymer (mol%)^b	The composition of the copolymer^a
MA–SMA-1	90	1.53×10^4	1.54	51.12	P(SMA-alt-MA)$_{35}$
MA–SMA-2	180	3.02×10^4	1.61	58.64	P(SMA-alt-MA)$_{50}$-PSMA$_{25}$
MA–SMA-3	360	3.18×10^4	1.65	59.88	P(SMA-alt-MA)$_{50}$-PSMA$_{30}$

[a] Determined by GPC
[b] Calculated by ^{1}H NMR analysis (400 MHz)

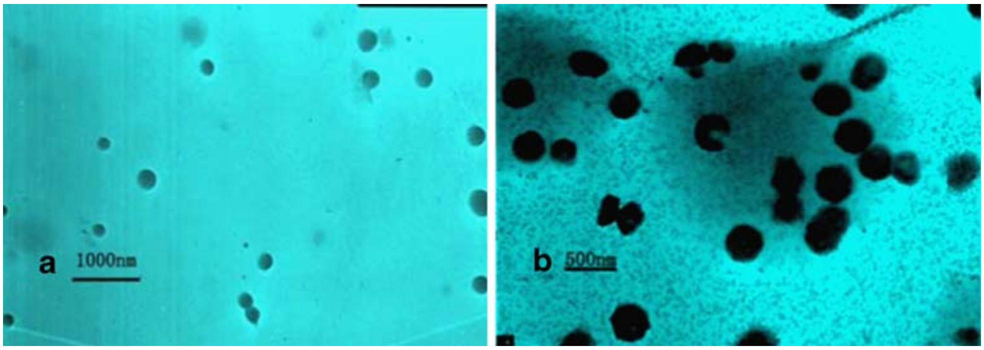

Fig. 4 TEM pictures of the aggregates from P(SMA-*alt*-MA)$_{50}$-*b*-PSMA$_{30}$ at various polymer concentrations in THF/water 90:10 (*w*/*w*). Polymer concentrations: 0.05 wt.% (**a**), 0.2 wt.% (**b**)

(633 nm). The scattering angle used for the measurements was 90°. A refractive index matching bath of filtered decalin surrounded the scattering cell, and the temperature was controlled usually at 30 °C. All the glass vessels were cleaned with detergent and rinsed abundantly with water and dried at 60 °C.

Results and discussion

Synthesis and characterization of BTBA and RAFT polymerization of MA and SMA using BTBA as chain transfer agent

Synthesis of chain transfer agent BTBA and the synthetic strategy followed for a novel comb-like amphiphilic copolymer [P(MA-*alt*-SMA)-*b*-PSMA] via the RAFT polymerization are depicted in Scheme 1.

As with other living radical polymerization methods [38], the RAFT polymerization offers block copolymers and allows for control of the molecular weight and narrow molecular weight distribution. The RAFT polymerizations of SMA and MA were carried out in these sealed tubes using BTBA as chain transfer agent at certain temperatures at a prescribed time interval; the results are shown in Figs. 1, 2, and 3 and in Table 1. It was found that MA–SMA copolymers with relatively narrow polydispersity ($1.54<M_w/M_n<1.65$) could be synthesized successfully by the RAFT polymerization.

As shown in Fig. 1, the chemical structures of the prepared products were characterized by ^{1}H NMR analysis. The ^{1}H NMR spectrum of BTBA showed peaks with the following shifts [37]: 4.60 (s, 2H), 7.28–7.60 (m, 8H), and 8.02 (m, 2H). The NMR spectrum of the product indicated that BTBA was successfully prepared.

The ^{1}H NMR spectrum of the MA–SMA copolymer showed peaks with the following shifts [39]: 0.88 [3H, in $CH_3(CH_2)_{15}$–], 0.86 and 0.90 (3H, in CH_3C–), 1.25 [30H, in –$(CH_2)_{15}CH_3$], 1.60 [2H, in –$CH_2(CH_2)_{15}CH_3$], 1.88 (2H, in –CH_2C), 2.73 (2H, in –*CH*–*CH*–), and 3.93 (2H, in –OCH_2–). The NMR spectrum of the product indicated that there existed SMA and MA moieties in the prepared copolymer.

Moreover, it was apparent in Fig. 2 that each of the GPC curves only showed a single peak; this result demonstrated that the possibility of the blend of PMA and PSMA could be excluded, and we further deduced that the resultant polymer may be a comb-like block copolymer P(MA-*alt*-MA)-*b*-PSMA.

To further reveal the alternating nature of the MA–SMA copolymer and the block nature of P(MA-*alt*-SMA)-*b*-PSMA, the RAFT polymerizations of MA and SMA with a molar feed of 1:4 were demonstrated at 60 °C after reaction for 90, 180, and 360 min, respectively. As shown in Table 1, it was found that the mole content of MA and

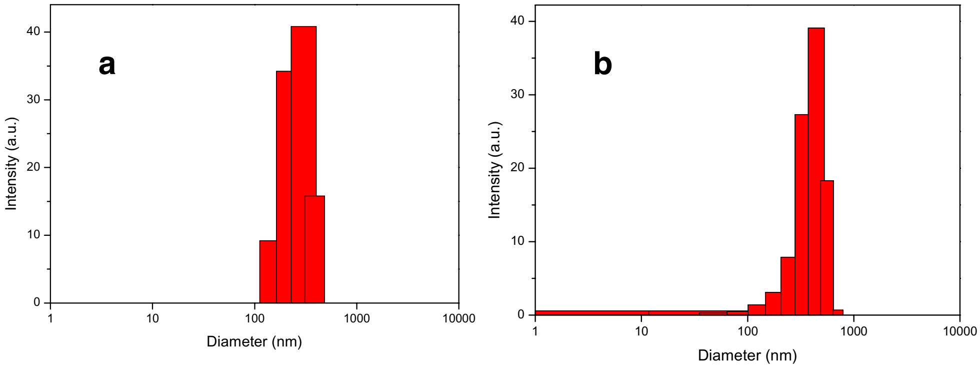

Fig. 5 Size distribution histograms of the aggregates from P(SMA-*alt*-MA)$_{50}$-*b*-PSMA$_{30}$ at various polymer concentrations in THF/H$_2$O 90:10 (*w*/*w*). Polymer concentrations: 0.05 wt.% (**a**), 0.20 wt.% (**b**)

Scheme 2 Schematic model of large spheres at various polymer concentrations

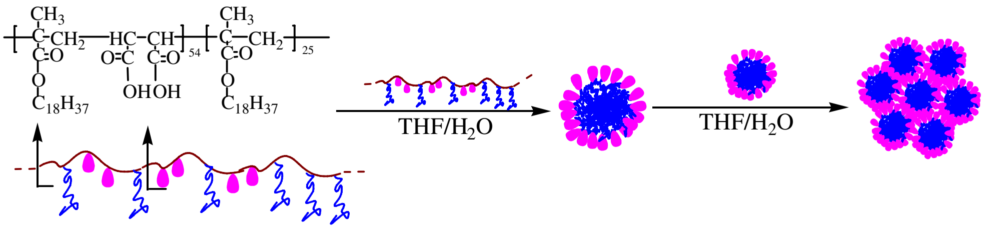

SMA in the copolymer was approximately equal during reaction for 90 min regardless of the large excess of SMA presented in the monomer feed under the RAFT polymerization conditions. With the reaction time, the mole content of SMA in the copolymer increased to 57.64 and 58.88%, respectively. Moreover, we investigated the change of conversion for MA and SMA monomers and their consumed molar ratio ($F_{\mathrm{SMA}}/F_{\mathrm{MA}}$) with the polymerization time via the RAFT polymerization. As shown in Fig. 3, the conversion of MA apparently increased faster than that of SMA; however, the absolute consumption of MA was approximately equal to that of SMA before MA was completely consumed (during reaction for 90 min). This further illuminated that this copolymer possessed an alternating structure before MA was completely exhausted. After MA was exhausted, the consumed molar ratio ($F_{\mathrm{SMA}}/F_{\mathrm{MA}}$) was beyond 1 and the conversion of SMA increased, which indicated that the alternating copolymer chain subsequently continued to propagate a PSMA block [27]. As a result, this further demonstrated that the unique diblock structure of the copolymer with an alternating block and a homopolymer block should be synthesized.

According to previous studies [27, 40], the possible mechanism of this polymerization can be deduced as follows: The predominantly alternating character was obtained at any monomer conversion due to the polar effect before MA had been exhausted [33]. It is the concept of the polar effect in free-radical chemistry that electron-rich radicals prefer to react with electron-poor substrates and vice versa. In this system, MA was a strongly electron-accepting monomer and SMA was an electron donor monomer, so strong electron donation in the comonomer would result in the alternating structure under the selected conditions. After MA was completely consumed, the consumption of essentially pure SMA continued chain propagation, which afforded a diblock copolymer with a PSMA block. In other words, the alternating copolymer chain subsequently continued to propagate, forming a block copolymer with SMA sequence.

Thus, a novel comb-like amphiphilic copolymer P(MA-*alt*-SMA)-*b*-PSMA could be obtained via the RAFT polymerization.

Self-assembly behaviors of P(MA-*alt*-SMA)-*b*-PSMA

It is known that the morphology of aggregates is a function of several factors, including the polymer concentration, water content, pH, temperature, and so on. All of these factors and the interplay between them influence the observed morphologies. In the present paper, we discussed mainly the effects of the polymer concentration, water content, and pH on the morphologies of P(MA-*alt*-SMA)-*b*-PSMA aggregates.

P(MA-*alt*-SMA)-*b*-PSMA could easily be hydrolyzed into its corresponding amphiphile, which could form uniform nanoscale particles in selective solvents by the self-assembly process [27]. These architectural particles in nanoscale size were of interest in further chemical or biological modification because they provided reactive or carboxylic groups on the surface of particles.

When THF and water were used as the common solvent and precipitant, respectively, the polymer concentration was a versatile parameter to adjust the morphologies of the aggregates. As shown in Fig. 4, the morphological change of P(MA-*alt*-SMA)$_{50}$-*b*-PSMA$_{30}$ was observed with the polymer concentration increasing at a water content of 10.0 wt.%. When the polymer concentration was 0.05 wt.%, spherical aggregates with average diameters of ca. 150–

Fig. 6 TEM pictures of the aggregates from P(SMA-*alt*-MA)$_{50}$-*b*-PSMA$_{30}$ at various water contents at the polymer concentration of 0.1 wt.% in THF/water. Water content: 5.0 wt.% (**a**), 10.0 wt.% (**b**), 30.0 wt.% (**c**)

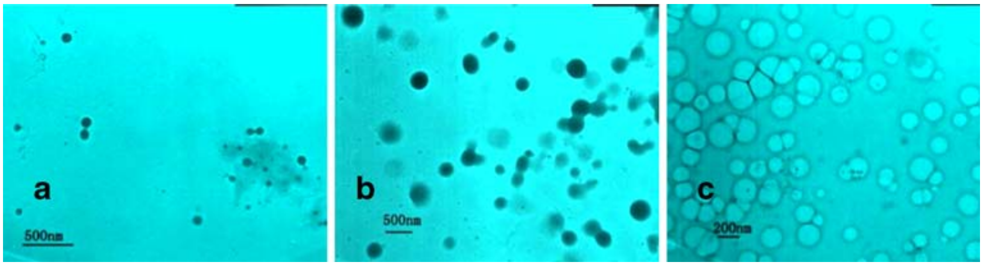

Fig. 7 Size distribution histograms of the aggregates from P(SMA-*alt*-MA)$_{50}$-*b*-PSMA$_{30}$ at various water contents at the polymer concentration of 0.1 wt.%. Water content: 5.0 wt.% (**a**), 10.0 wt.% (**b**), 30.0 wt.% (**c**)

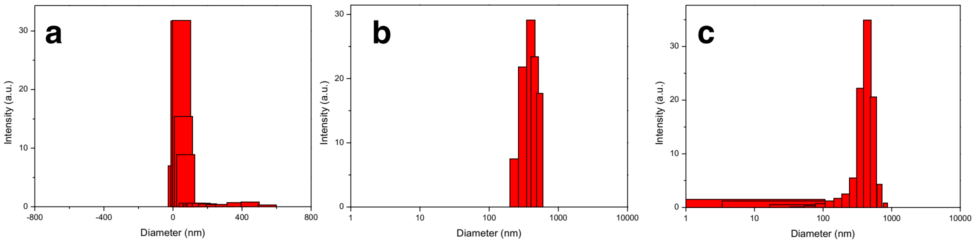

200 nm were observed (Fig. 4a). With a further increase in the polymer concentration to 0.2 wt.%, large spherical aggregates with average diameters of ca. 400 nm coexisting with small alone spheres had been found (Fig. 4b). Furthermore, the dimension of these aggregates at the above conditions was also examined by dynamic light scattering (DLS), and the data are shown in Fig. 5. The results indicated that the average sizes of these aggregates were about 250 and 480 nm, respectively, which were a little larger than those observed by TEM because the corona (the maleic acid units) of the aggregates would stretch out to some degree in the solution, while TEM observation showed the dried aggregates [8]. Considering the chemical structure of P(MA-*alt*-SMA)$_{50}$-*b*-PSMA$_{30}$, the dimension of these aggregates was very large. If the polymer chains would stretch out in the solution, the diameter of these aggregates should not exceed $(54 \times 2 + 25) \times 2 \times 0.25\ nm = 66.5\ nm$. Thus, these aggregates were not simple spheres, and some MA units must be located inside the core of the aggregates. Consequently, the large spherical aggregate was ascribed to large compound micelles [41].

It is well known that the self-assembly of amphiphile in selective solvents can result in the formation of various morphologies [42, 43]. In the present study, the formation of large spheres in THF/water led us to suggest the following model for the self-assembly behavior (Scheme 2). P(MA-*alt*-SMA)$_{50}$-*b*-PSMA$_{30}$ was first dissolved in THF, which was suitable for both blocks, and then water, which was a precipitant for PSMA comb-like blocks while simultaneously a good solvent for the maleic acid units, was added into the solution. The PSMA blocks would associate to form simple spherical micelles because of the attractive forces between P(MA-*alt*-SMA)$_{50}$-*b*-PSMA$_{30}$ and the repulsive forces preventing the initial growth of the aggregate at the low concentration. With the polymer concentration increasing, the aggregate number must increase correspondingly. The higher aggregate number should result in the collision of the aggregates with each other by Brownian motion in the solution. The shell–solvent interaction could not stabilize the spherical aggregates any longer because the soluble maleic acid units were very short, so more amphiphilic molecules were needed to associate together to improve the shell–solvent interaction and stabilize the aggregates in selective solvents. Consequently, the maleic acid units flocculated or interpenetrated to form the continuous phase while the insoluble PSMA blocks were pocketed by the maleic acid units. Therefore, large spheres would form by undergoing a secondary aggregation during the self-assembly process.

Water content also plays an important role in the self-assembly process. Figure 6 showed that P(MA-*alt*-SMA)$_{50}$-*b*-PSMA$_{30}$ aggregates exhibited various morphologies at different water contents at the polymer concentration of 0.1 wt.% in THF/water. The spherical aggregates with average diameters of ca. 50–100 nm were found at water content of 5.0 wt.% (Fig. 6a). As water content increased to 10.0 wt.%, as shown in Fig. 6b, large spheres with average diameters of ca. 250–400 nm were formed. With a further increase in water content to 30.0 wt.%, a monolayer film with some pores was seen in Fig. 6c. DLS was also used to investigate the aggregation behavior of P(MA-*alt*-SMA)$_{50}$-*b*-PSMA$_{30}$ in THF/water. As shown in Fig. 7, the diameters of these aggregates were larger than those measured by TEM (Fig. 7), and the results were similar to what have been found in the above section.

According to previous studies [44], the possible mechanism of the morphological transition from individual small spheres to large spherical aggregates and the monofilm with a few pores was ascribed to various water contents in THF/water (Scheme 3). When water was added to the self-assembly solution, the increase in the interfacial energy between the core of the aggregates and the solvent resulted

Scheme 3 Schematic model of the aggregates at various water contents

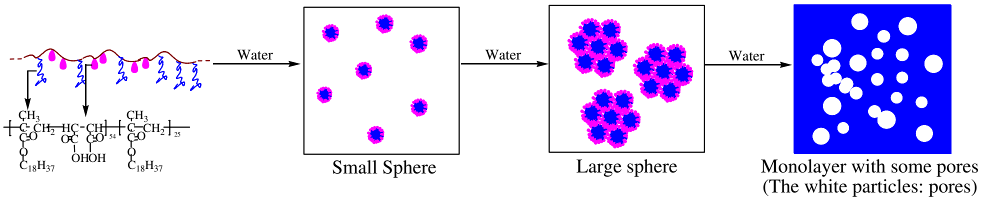

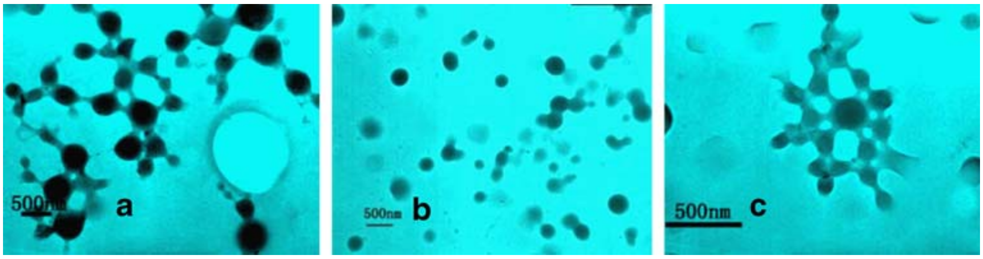

Fig. 8 TEM pictures of the aggregates from P(SMA-*alt*-MA)$_{50}$-*b*-PSMA$_{30}$ at various pH values at the polymer concentration of 0.1 wt.% in THF/water 90:10 (*w*/*w*). pH 4.0 (**a**), 5.8 (**b**), 12.0 (**c**)

in the increase in the aggregate number. Thus, the effect of water content on the morphology would be similar to that of the polymer concentration during the self-assembly process [44]. It could be found that the morphologies in Fig. 6a,b were similar to those in Fig. 4a,b. With a further increase in water content, the aggregate number had to increase, which led to the enhancement of the aggregate dimension by undergoing a secondary aggregation. When the larger soft particles transfer to the carbon-coated copper grid, they must collapse due to the removal of the solvent and form a monolayer. In addition, the volatilization of solvent resulted in the formation of some pores in the monofilm. As a result, a monolayer film with some pores was formed.

The pH of the water phase is a versatile tool to adjust the structures of aggregates. Figure 8 shows a set of typical TEM pictures of P(MA-*alt*-SMA)$_{50}$-*b*-PSMA$_{30}$ aggregates made in different pH values of the water phase at the polymer concentration of 0.1 wt.% in THF/water 90:10 (*w*/*w*). Without the addition of HCl or NaOH to the solution, the copolymer yielded spheres of low polydispersity with average diameters of 250–400 nm (Fig. 8b). When HCl was added to the solution and the pH value was changed to 4, the aggregates were still spheres with average diameters of 600 nm (Fig. 8a). However, when NaOH was used and the pH value of the solution was converted into 12, it was of great interest that the morphology changed in the opposite direction from what was seen at the pH value of 4, and the aggregates were still spheres with smaller size (Fig. 8c). Figure 9 shows the dimensions of aggregates at various pH values in THF/water; the data measured by DLS supported the results observed by TEM (Fig. 8).

According to previous studies [44–47], when P(MA-*alt*-SMA)$_{50}$-*b*-PSMA$_{30}$ was easily hydrolyzed into the corresponding amphiphile in THF/water, we knew that the maleic acid segments were partially ionized because water was distributed around them. In the present system, when HCl was added to the self-assembly solution, some of the ionized carboxylic acidic units of the maleic acid segments were protonated, which led to the decrease in the electrostatic repulsion among the corona chains. Consequently, the stretching degree of the core chains (the PSMA chains) must increase correspondingly, which resulted in the increase in the aggregate size. However, with the addition of NaOH (aq), the maleic acid units became deprotonated, which led to an increase in the degree of ionization of maleic acid. As a result, the electrostatic repulsion among the corona chains must increase, so the morphology was found to change in the opposite direction, i.e., from large spheres to small ones with the pH value increasing.

Conclusions

In this paper, a novel comb-like block copolymer having alternating segments P(MA-*alt*-SMA)-*b*-PSMA was successfully synthesized using the RAFT polymerization. The aggregation behaviors of P(MA-*alt*-SMA)-*b*-PSMA were investigated in THF/water. It is of great interest that the aggregates with different morphologies and dimensions could be obtained easily by adjusting the polymer concentration, water content, and pH. The resulting aggregates show new potential applications in the field of biomaterials, drug delivery systems, and so on because they provide reactive or carboxylic groups on their surfaces.

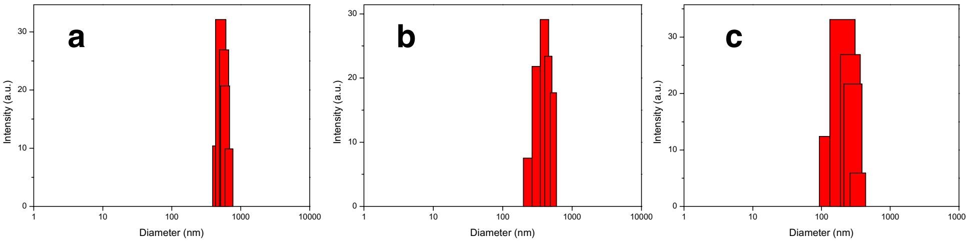

Fig. 9 Size distribution histograms of the aggregates from P(SMA-*alt*-MA)$_{50}$-*b*-PSMA$_{30}$ at various pH values at polymer concentrations of 0.1 wt.% in THF/H$_2$O 90/10 (*w*/*w*). pH 4.0 (**a**), 5.8 (**b**), 12.0 (**c**)

References

1. Price C, Woods D (1973) Eur Polym J 9:827
2. Price C (1983) Pure Appl Chem 55:1563
3. Pedersen JS, Svaneborg C (2002) Curr Opin Colloid Interface Sci 7:158
4. Shen H, Eisenberg A (2000) Angew Chem Int Ed Engl 39:3310
5. Zhulina EB, Borisov OV (2002) Macromolecules 35:9191
6. Kataoka K, Harada A, Nagasaki Y (2001) Adv Drug Deliv Rev 47:113
7. Eisenberg A (1998) Chem Mater 10:1021
8. Zhou JF, Wang L, Wang CL, Chen T, Yu HJ, Yang Q (2005) Polymer 46(24):11157
9. Yu HJ, Wang L, Zhou JF, Jiang GH, Zhao ZR (2006) J Phys Chem B 110:837
10. Zhou JF, Wang L, Chen T, Wang W (2005) Prog Chem 17(6):1102
11. Zhou JF, Wang L, Dong XC, Chen T, Yang Q, Chen C, Chen X (2006) Nanotechnology 17:2745
12. Riess G (2003) Prog Polym Sci 28(7):1107
13. Rosler A, Vandermeuler GWM, Klok HA (2001) Adv Drug Deliv Rev 53:95
14. Allen C, Maysinger D, Eisenberg A (1999) Colloids Surf B Biointerfaces 16:3
15. Borisov OV, Zhulina EB (2002) Macromolecules 35:4472
16. Moffitt M, Eisenberg A (1997) Macromolecules 30:4363
17. Zhao H, Douglas EP, Harrison BS, Schanze KS (2001) Langmuir 17:8428
18. Shen H, Eisenberg A (1999) J Phys Chem B 103:9473
19. Riegel IC, Samios D, Petzhold CL, Eisenberg A (2003) Polymer 44:2117
20. Luo L, Eisenberg A (2002) Angew Chem Int Ed Engl 41:1001
21. Burke SE, Eisenberg A (2001) Langmuir 17:8341
22. Croll LM, Stover HDH (2003) Langmuir 19:10077
23. Ray B, Isobe Y, Morioka K, Habaue S, Okamoto Y, Kamigaito M, Sawamoto M (2003) Macromolecules 36(3):543
24. Parrish B, Emrick T (2004) Macromolecules 37(16):5863
25. Baum M, Brittain WJ (2002) Macromolecules 35(3):610
26. Feng XS, Pan CY (2002) Macromolecules 35(13):4888
27. Zhu MQ, Wei LH, Li M, Jiang L, Du FS, Li ZC, Li FM (2001) Chem Commun 365
28. Li FM, Zhu MQ, Zhang X, Wei LH, Du FS, Li ZC (2003) Acs Symp Ser 854:342
29. Davies MC, Dawkins JV, Hourston DJ (2005) Polymer 46:1739
30. Chernikova E, Terpugova P, Bui C, Charleux B (2003) Polymer 44:4101
31. Pitsikalis M, Siakali-Kioulafa E, Hadjichristidis N (2000) Macromolecules 33:5460
32. Xu B, Li L, Zhang K, Macdonald PM, Winnik MA, Jenkins R, Bassett D, Wolf D, Nuyken O (1997) Langmuir 13(26):6896
33. van der Linden CC, Leermakers FAM, Fleer GJ (1996) Macromolecules 29(3):1000
34. Gargallo L, Leiva A, Urzua M, Alegria L, Miranda B, Radic D (2004) Polym Int 53(11):1652
35. Gargallo L, Miranda B, Leiva A, Radic D (2001) Polimery 46(11–12):828
36. Qin S, Saget J, Pyun J, Jia S, Kowalewski T, Matyjaszewski K (2003) Macromolecules 36:8969
37. Moad G, Chiefari J, Chong JK, Kristina J, Mayadunne RTA, Rizzardo E, Thang SH (2000) Polym Int 49:993
38. Jiang GH, Wang L, Chen T, Yu HJ (2005) Polymer 46:81
39. Song Y, Ren T, Fu X, Xu X (2005) Fuel Process Technol 86:641
40. Hall HK, Padias AB (2001) J Polym Sci A Polym Chem 39:2069
41. Zhang Y, Luo S, Liu S (2005) Macromolecules 38:9813
42. Zhang L, Eisenberg A (1996) J Am Chem Soc 118(13):3168
43. Ravi P, Dai S, Tan CH, Tam KC (2005) Macromolecules 38 (3):933
44. Zhang L, Eisenberg A (1998) Polym Adv Technol 9:677
45. Zhang L, Eisenberg A (1999) Macromolecules 32(7):2239
46. Zhang L, Eisenberg A (1996) Macromolecules 29(27):8805
47. Zhang L, Shen H, Eisenberg A (1997) Macromolecules 30 (4):1001